

1 **Transmission dynamics and control of COVID-19 in Chile, March-October, 2020**

2

3 Anna Tariq<sup>1\*</sup>, Eduardo A. Undurraga<sup>2,3</sup>, Carla Castillo Laborde<sup>4</sup>, Katia Vogt-Geisse<sup>5</sup>, Ruiyan Luo<sup>1</sup>,

4 Richard Rothenberg<sup>1</sup>, Gerardo Chowell<sup>1</sup>

5

6 1 Department of Population Health Sciences, School of Public Health, Georgia State University, Atlanta,

7 GA, USA

8 2 Escuela de Gobierno, Pontificia Universidad Católica de Chile, Santiago, RM, Chile

9 3 Millennium Initiative for Collaborative Research in Bacterial Resistance (MICROB-R), Santiago, RM,

10 Chile

11 4 Centro de Epidemiología y Políticas de Salud, Facultad de Medicina, Clínica Alemana Universidad del

12 Desarrollo, Santiago, RM, Chile

13 5 Facultad de Ingeniería y Ciencias, Universidad Adolfo Ibáñez, Santiago, RM, Chile

14

15 \* Correspondence: Anna Tariq, Department of Population Health Sciences, Georgia State University

16 School of Public Health, Atlanta, GA, 30303, atariq1@student.gsu.edu; Tel.: 470-985-6352

17

18

19

## 20 **Abstract**

21 Since the detection of the first case of COVID-19 in Chile on March 3<sup>rd</sup>, 2020, a total of 513188 cases,  
22 including ~14302 deaths have been reported in Chile as of November 2<sup>nd</sup>, 2020. Here, we estimate the  
23 reproduction number throughout the epidemic in Chile and study the effectiveness of control  
24 interventions especially the effectiveness of lockdowns by conducting short-term forecasts based on the  
25 early transmission dynamics of COVID-19. Chile's incidence curve displays early sub-exponential  
26 growth dynamics with the deceleration of growth parameter,  $p$ , estimated at 0.8 (95% CI: 0.7, 0.8) and the  
27 reproduction number,  $R$ , estimated at 1.8 (95% CI: 1.6, 1.9). Our findings indicate that the control  
28 measures at the start of the epidemic significantly slowed down the spread of the virus. However, the  
29 relaxation of restrictions and spread of the virus in low-income neighborhoods in May led to a new surge  
30 of infections, followed by the reimposition of lockdowns in Greater Santiago and other municipalities.  
31 These measures have decelerated the virus spread with  $R$  estimated at ~0.96( 95% CI: 0.95, 0.98) as of  
32 November 2<sup>nd</sup>, 2020. The early sub-exponential growth trend ( $p \sim 0.8$ ) of the COVID-19 epidemic  
33 transformed into a linear growth trend ( $p \sim 0.5$ ) as of July 7<sup>th</sup>, 2020, after the reimposition of lockdowns.  
34 While the broad scale social distancing interventions have slowed the virus spread, the number of new  
35 COVID-19 cases continue to accrue, underscoring the need for persistent social distancing and active case  
36 detection and isolation efforts to maintain the epidemic under control.

37

## 38 **Author summary**

39 In context of the ongoing COVID-19 pandemic, Chile has been one of the hardest-hit countries in Latin  
40 America, struggling to contain the spread of the virus. In this manuscript, we employ renewal equation to  
41 estimate the reproduction number ( $R$ ) for the early ascending phase of the COVID-19 epidemic and by  
42 July 7<sup>th</sup>, 2020 to guide the magnitude and intensity of interventions required to combat the COVID-19  
43 epidemic. We also estimate the instantaneous reproduction number throughout the epidemic in Chile.  
44 Moreover, we generate short-term forecasts based on the epidemic trajectory using phenomenological

45 models, and assess counterfactual scenarios to understand any additional resources required to contain the  
46 virus' spread. Our results indicate early sustained transmission of SARS-CoV-2. However, the initial  
47 control measures at the start of the epidemic significantly slowed down the spread of the virus. The easing  
48 of COVID-19 restrictions in April led to a new wave of infections, followed by the re-imposition of  
49 lockdowns in Greater Santiago and other municipalities. Most recent estimates of reproduction number  
50 indicate a decline in the virus transmission. While broad-scale social distancing interventions have slowed  
51 the virus spread, the number of new COVID-19 cases continue to accrue, underscoring the need for  
52 persistent social distancing efforts.

53

54

## 55 **Introduction**

56 The coronavirus disease 2019 (COVID-19), caused by severe acute respiratory syndrome coronavirus 2  
57 (SARS-CoV-2), was declared a global pandemic by the World Health Organization (WHO) on March  
58 11<sup>th</sup>, 2020 [1, 2]. This highly contagious unprecedented virus has impacted government and public  
59 institutions, strained the health care systems, restricted people in their homes, and caused country-wide  
60 lockdowns resulting in a global economic crisis [3-5]. Moreover, as of November 2<sup>nd</sup>, 2020, nearly 46  
61 million COVID-19 cases in 213 countries and territories have been reported, including more than 1.2  
62 million deaths [6]. The social, economic, and psychological impact of this pandemic on much of the  
63 world's population is profound [7-13].

64  
65 Soon after its initial rapid spread in China, the first case of novel coronavirus beyond China was reported  
66 in Thailand on January 13<sup>th</sup>, 2020 [14]. The first case in the USA was not identified until January 20<sup>th</sup>,  
67 2020 followed by the detection of the first cases in the European territory on January 24<sup>th</sup>, 2020 [15, 16].  
68 The COVID-19 pandemic has since spread to every continent except the Antarctica. While some  
69 countries like New Zealand and Australia have steadily suppressed the COVID-19 spread, reporting less  
70 than 150 cases per day as of November 2<sup>nd</sup>, 2020, other countries like Brazil, India, and the USA still  
71 struggle to contain the increasing number of cases [17]. Subsequently, considerable COVID-19 outbreaks  
72 have occurred in Latin America since late February 2020.

73  
74 The WHO declared Latin America the new epicenter of the COVID-19 on May 22<sup>nd</sup>, 2020 [18]. Latin  
75 America has paid a high toll during the COVID-19 pandemic, with some of the worlds' highest death  
76 rates [19-21]. While home to less than 10% of the world population, Latin America accounts for about  
77 one-third of all reported global deaths (~370 thousand) [6]. Several socioeconomic, demographic, and  
78 political factors make control of the pandemic in Latin America particularly challenging [22-25]. Most  
79 countries in the region are now facing the stark social and economic costs imposed by large-scale non-

80 pharmaceutical interventions while largely failing to control the epidemic's spread [13, 24, 26]. Despite  
81 these unique conditions, the region has received relatively little attention from researchers globally [19].  
82 As of November 1<sup>st</sup>, 2020, the highest number of cases have been reported in Brazil (5,516,658), followed  
83 by Argentina (1,157,179), Colombia (1,063,151), Mexico (918,811), Peru (900,180) and Chile (510,256)  
84 [17, 27]. Adjusted by population, Chile's COVID-19 outbreak is among the worst globally, with more  
85 than 26,000 cases and 980 deaths per million inhabitants [28].

86

87 The first case of SARS-CoV-2 in Chile was identified on March 3<sup>rd</sup>, 2020. While the initial cases were  
88 imported from southeast Asia and Europe, the COVID-19 case counts have expanded in this country,  
89 placing Chile in phase 4 of the pandemic on March 25<sup>th</sup>, 2020 [28, 29]. Chile was the fifth country in  
90 Latin America after Brazil, Mexico, Ecuador and Argentina to report COVID-19 cases. The first six  
91 imported cases were reported in Talca and in the capital of Chile, Santiago [28]. However, since the early  
92 phase of the outbreak, Chile has employed an agile public health response by announcing a ban on public  
93 health gatherings of more than 500 people on March 13<sup>th</sup>, 2020, when the nationwide cumulative case  
94 count reached 44 reported cases [30].

95

96 Moreover, the Chilean government announced the closure of all daycares, schools, and universities on  
97 March 16<sup>th</sup>, 2020. These closures were followed by the announcement to close country borders on March  
98 18<sup>th</sup>, 2020, and the declaration of national emergency on the same date, accompanied by several concrete  
99 interventions to further contain the outbreak in the region [31]. In particular, these included a night-time  
100 curfew in Chile starting on March 22<sup>nd</sup>, 2020, and localized lockdowns (i.e., intermittent lockdowns at the  
101 municipality level depending on total cases and case growth) starting on March 28<sup>th</sup>, 2020 in two  
102 municipalities in Southern Chile and seven municipalities in Santiago [32]. These initial containment  
103 strategies kept the COVID-19 case counts lower than regional peers; Brazil, Peru, and Ecuador until the  
104 end of April 2020. However, the government started to ease the COVID-19 restrictions in late April by  
105 reopening the economy under the "Safe Return" plan, including the televised opening of some businesses

106 and stores, as new infections had reduced between 350-500 per day by the end of April, implying an only  
107 apparent flattening of the COVID-19 curve [33-35]. Moreover, imposing and lifting lockdowns in small  
108 geographical areas (municipalities) proved unsuccessful in areas with high interdependencies such as the  
109 Greater Santiago [36] . This strategy resulted in a new wave of infections; with the virus spreading from  
110 more affluent areas of Chile to more impoverished, crowded communities, forcing the government to  
111 reimpose lockdown measures in Santiago in mid-May (Figure 1) [23, 37, 38]. By mid-July, the  
112 government implemented the “step by step” strategy, considering five stages of gradual opening, at the  
113 municipality level, based on the periodic monitoring of epidemiological and health system indicators. The  
114 case counts continued to increase, averaging ~4943 cases per day in June 2020, and started to decline  
115 thereafter. The mid-June peak of infections resulted in intensive care units (ICU) reaching saturation  
116 levels of 89% nationally and 95% in the Metropolitan Region [39]. Thus far, Chile has accumulated  
117 513,188 reported cases including 14,302 deaths as of November 2<sup>nd</sup>, 2020. The majority (~52%) of  
118 COVID-19 cases are concentrated in Region Metropolitana (mostly in Chile’s capital, Santiago), with  
119 297,423 reported cases, followed by 30,498 cases in Valparaiso located in coastal central Chile, and  
120 30,934 cases in Biobio located in southern Chile [40, 41]. Moreover, the crude case fatality rate in Chile  
121 (~2.8%) resonates with the global average case fatality rate (2.6%) [17, 42].

122  
123 In this study, we estimate the transmission potential of COVID-19, including the effective reproduction  
124 number,  $R$ , during the early transmission phase of the COVID-19 epidemic in Chile and around the mid  
125 of the epidemic, by July 7<sup>th</sup>, 2020. We also estimate the instantaneous reproduction number throughout  
126 the epidemic in Chile. The reproduction number can guide the magnitude and intensity of control  
127 interventions required to combat the COVID-19 outbreak [43, 44]. We examine the effectiveness of  
128 control interventions in Chile (see Table 1) on the transmission rate. To do this, we conduct short-term  
129 forecasts using phenomenological growth models calibrated using the early trajectory of the epidemic and  
130 by the mid of the epidemic (as of July 7<sup>th</sup>, 2020) [45] to anticipate additional resources required to contain  
131 the epidemic. These phenomenological growth models are useful in capturing the epidemic’s empirical

132 patterns, especially when the epidemiological data are limited, and significant uncertainty exists around  
133 infectious disease epidemiology [46]. These models provide a starting point for forecasting the epidemic  
134 size and characterizing the temporal changes in the reproduction number during the epidemic [47].

135

136 Figure 1: Timeline of the milestones of the COVID-19 pandemic in Chile as of November 2<sup>nd</sup>, 2020.

137

138 Table 1: Timeline of the implementation of the social distancing interventions in Chile as of November  
139 2<sup>nd</sup>, 2020.

140

<b>Date</b>	<b>Control interventions</b>
March 13 <sup>th</sup> , 2020	Ban on large social gatherings implemented in Chile [30]
March 16 <sup>th</sup> , 2020	Closures of daycares, schools, and universities in Chile [32, 48]  Mandatory quarantine of high-risk individuals returning from Iran, China, West Europe and South Korea
March 18 <sup>th</sup> , 2020	Declaration of national emergency (14)  Closure of country borders (14)  Telework implemented
March 19 <sup>th</sup> , 2020	Closure of mall and department stores with the exception of supermarkets, pharmacies, banks and grocery stores
March 21 <sup>st</sup> , 2020	Closure of non-essential business including theatres, restaurant, bars and gyms

March 22 <sup>nd</sup> , 2020	Night time curfew implemented [32]
March 26 <sup>th</sup> , 2020	Intermittent lockdown initiated (implemented at municipality level) [32]
April 8 <sup>th</sup> , 2020	Orders on mandatory use of facemasks in public transport [49]
April 17 <sup>th</sup> , 2020	Orders on mandatory use of facemasks in all public spaces [60]
April 30 <sup>th</sup> , 2020	First shopping mall is reopened in Santiago and then closed the next day [50]
May 5 <sup>th</sup> , 2020	Total lockdown in Antofagasta [31]
May 15 <sup>th</sup> , 2020	Total lockdown imposed in all municipalities of Santiago [51]
June 12 <sup>th</sup> , 2020	Total lockdown in Valparaiso [31]
July 19 <sup>th</sup> , 2020	Step by step gradual reopening of the country

141

## 142 **Methods**

### 143 **COVID-19 incidence and testing data**

144 We obtained updates on the daily series of new COVID-19 cases as of November 2<sup>nd</sup>, 2020, from the  
145 publicly available data from the GitHub repository created by the Chile's government [27]. Incidence  
146 case data by the date of reporting per day, confirmed by PCR (polymerase chain reaction) tests from  
147 March 3<sup>rd</sup>–November 2<sup>nd</sup>, 2020, were analyzed. The daily testing and positivity rates available from April  
148 9<sup>th</sup>–November 2<sup>nd</sup>, 2020, were also analyzed.

149

### 150 **Models**



151 We utilize two phenomenological growth models, the generalized growth model (GGM) and the  
152 generalized logistic growth model (GLM) that have been validated by deriving short-term forecasts for  
153 multiple infectious diseases in the past, including SARS, pandemic Influenza, Ebola, and Dengue [52,  
154 53].

155

### 156 **Generalized growth model (GGM)**

157 We generate short term forecasts using the generalized growth model (GGM) that characterizes the early  
158 ascending phase of the epidemic by estimating two parameters: (1) the intrinsic growth rate,  $r$ ; and (2) a  
159 dimensionless “deceleration of growth” parameter,  $p$ . This model allows to capture a range of epidemic  
160 growth profiles by modulating parameter  $p$ . The GGM model is given by the following differential  
161 equation:

$$\frac{dC(t)}{dt} = C'(t) = rC(t)^p$$

162 In this equation  $C'(t)$  describes the incidence curve over time  $t$ ,  $C(t)$  describes the cumulative number of  
163 cases at time  $t$  and  $p \in [0,1]$  is a “deceleration of growth” parameter. This equation becomes constant  
164 incidence over time if  $p=0$  and an exponential growth model for cumulative cases if  $p=1$ . Whereas if  $p$  is  
165 in the range  $0 < p < 1$ , then the model indicates sub-exponential growth dynamics [54, 55].

166

### 167 **Generalized logistic growth model (GLM)**

168 The generalized logistic growth model (GLM) is an extension of the simple logistic growth model that  
169 captures a range of epidemic growth profiles, including sub-exponential (polynomial) and exponential  
170 growth dynamics. GLM characterizes epidemic growth by estimating (i) the intrinsic growth rate,  $r$  (ii) a  
171 dimensionless “deceleration of growth” parameter,  $p$  and (iii) the final epidemic size,  $k_0$ . The final  
172 epidemic size is sensitive to small variations in the deceleration of growth parameters [56] and would  
173 vary as the epidemic progresses. The deceleration parameter modulates the epidemic growth patterns,

174 including the sub-exponential growth ( $0 < p < 1$ ), constant incidence ( $p = 0$ ) and exponential growth  
175 dynamics ( $p = 1$ ). The GLM model is given by the following differential equation:

$$\frac{dC(t)}{dt} = rC^p(t)\left(1 - \frac{C(t)}{k_0}\right)$$

176 Where  $\frac{dC(t)}{dt}$  describes the incidence over time  $t$  and the cumulative number of cases at time  $t$  is given by  
177  $C(t)$  [45]. This simple logistic growth type model typically supports single peak epidemics in the number  
178 of new infections followed by a burnt-out period, unless external driving forces such as the seasonal  
179 variations in contact patterns exist. This model can underestimate the peak timing and the duration of  
180 outbreaks. This model can also underestimate the case incidence before the inflection point has occurred  
181 [45, 47, 53, 57].

182

### 183 **Calibration of the GGM and GLM model**

184 We calibrate the GGM and the GLM model to the daily incidence curve by dates of reporting in Chile  
185 using time series data from March 3<sup>rd</sup>–March 30<sup>th</sup>, 2020, and from May 9<sup>th</sup> – July 7<sup>th</sup>, 2020, respectively  
186 (Figure 2). The period from March 3<sup>rd</sup>–March 30<sup>th</sup>, 2020, includes the initial interventions made by the  
187 Chilean government, whereas the period from May 9<sup>th</sup>-July 7<sup>th</sup>, 2020, comprises the reimposition of  
188 lockdowns after a brief reopening of society under the “new normal” (Figure 1).

189

190 Model parameters are estimated by a non-linear least-square fitting of the model solution to the incidence  
191 data by the date of reporting. This is achieved by searching for the set of model parameters  $\hat{\Theta} =$   
192  $(\hat{\Theta}_1, \hat{\Theta}_2, \dots, \hat{\Theta}_m)$  that minimizes the sum of squared differences between the observed data  $y_{ti} =$   
193  $y_{t1}, y_{t2}, \dots, y_{tn}$  and the corresponding mean incidence curve given by  $f(t_i, \hat{\Theta}) = C'(t)$  : where  $\hat{\Theta} = (r, p)$   
194 corresponds to the set of parameters of the GGM model and  $\hat{\Theta} = (r, p, k_0)$  corresponds to the set of  
195 parameters of the GLM model. In both cases, the objective function for the best fit solution of  $f(t_i, \hat{\Theta})$  is  
196 given by :

197

198  $\hat{\Theta} = \arg \min \sum_{i=1}^n (f(t_i, \Theta) - y_{t_i})^2$

199

200 where  $t_i$  is the time stamp at which the time series data are observed and  $n$  is the total number of data  
201 points available for inference. The initial condition is fixed to the first observation in the data set. This  
202 way,  $f(t_i, \hat{\Theta})$  gives the best fit to the time-series data  $y_{t_i}$ . Next, we utilize a parametric bootstrapping  
203 approach assuming a negative binomial error structure for the GGM and GLM model to derive  
204 uncertainty in the parameters obtained by non-linear least-square fit of the data as previously described  
205 [54, 58]. The variance is assumed to be three times the mean for GGM and 96 times the mean for the  
206 GLM. The model confidence intervals of parameters and the 95% prediction intervals of model fit are  
207 also obtained using the parametric bootstrap approach [54].

208

### 209 **Reproduction number, $R$ , from case incidence using GGM**

210 The reproduction number,  $R$ , is defined as the average number of secondary cases generated by a primary  
211 case at time  $t$  during the outbreak. This is crucial to identify the intensity of interventions required to  
212 contain an epidemic [59-61]. Estimates of effective  $R$  indicate if the disease transmission continues ( $R > 1$ )  
213 or if the active disease transmission ceases ( $R < 1$ ). Therefore, in order to contain an outbreak, we need to  
214 maintain  $R < 1$ . We estimate the reproduction number by calibrating the GGM to the epidemic's early  
215 growth phase (27 days) [55]. We model the generation interval of SARS-CoV-2, assuming gamma  
216 distribution with a mean of 5.2 days and a standard deviation of 1.72 days [62]. We estimate the growth  
217 rate parameter,  $r$ , and the deceleration of growth parameter,  $p$ , as described above. The progression of  
218 local incidence cases  $I_i$  at calendar time  $t_i$  is simulated from the calibrated GGM model. Then in order to  
219 estimate the reproduction number, we apply the discretized probability distribution of the generation  
220 interval denoted by  $\rho_i$  to the renewal equation as follows [43, 44, 63]:

221

$$R_{t_i} = \frac{I_i}{\sum_{j=0}^i (I_{i-j} \rho_j)}$$

222

223 The numerator represents the total new cases  $I_i$ , and the denominator represents the total number of cases  
224 that contribute to generating the new cases  $I_i$  at time  $t_i$ . Hence,  $R_t$ , represents the average number of  
225 secondary cases generated by a single case at time  $t$ . Next, we derive the uncertainty bounds around the  
226 curve of  $R_t$  directly from the uncertainty associated with the parameter estimates ( $r, p$ ) obtained from the  
227 GGM. We estimate  $R_t$  for 300 simulated curves assuming a negative binomial error structure where the  
228 variance is assumed to be three times the mean [54].

229

### 230 **Reproduction number, $R$ , from case incidence using GLM**

231 In order to estimate the reproduction number by July 7<sup>th</sup>, 2020 (after the reimposition of lockdowns in  
232 Santiago and Valparaiso), we calibrate the GLM from May 9<sup>th</sup> – July 7<sup>th</sup>, 2020 [55]. Next, we model the  
233 generation interval [62], estimate the model parameters ( $r, p, k_0$ ) from GLM and the reproduction number  
234 from the renewal equation as described above [43, 44, 63]. The uncertainty bounds around the curve of  $R_t$   
235 are derived directly from the uncertainty associated with the parameter estimates ( $r, p, k_0$ ). We estimate  
236  $R_t$  for 300 simulated curves assuming a negative binomial error structure [54] where the variance is  
237 assumed to be 96 times of the mean calculated by averaging mean to variance ratio calculated from the  
238 data (by binning data points and calculating directly from the data itself).

239

### 240 **Instantaneous reproduction number, $R$ , using the Cori method**

241 We estimate  $R$  by the ratio of number of new infections generated at time  $t$  ( $I_t$ ), to the total infectiousness  
242 of infected individuals at time  $t$ , given by :

$$243 \quad \sum_{s=1}^t I_{t-s} w_s \text{ [64, 65]}$$

244 In this equation,  $w_s$  represents the infectivity profile of the infected individual, which depends on the time  
245 since infection ( $s$ ), but is independent of the calendar time ( $t$ ) [66, 67].

246

247 More specifically,  $w_s$  is defined as a probability distribution describing the average infectiousness profile  
248 of an individual after infection. Distribution of  $w_s$  is affected by individual biological factors such as  
249 symptom severity or pathogen shedding. The equation  $\sum_{s=1}^t I_{t-s} w_s$  indicates the sum of infection  
250 incidence up to time step  $t - 1$ , weighted by the infectivity function  $w_s$ . The distribution of the generation  
251 time can be utilized to approximate the infectivity profile,  $w_s$ , however, since the time of infection is  
252 rarely observed, it becomes difficult to measure the distribution generation time [64]. Hence, time of  
253 symptom onset is usually used to estimate the distribution of serial interval, which is defined as the time  
254 interval between the dates of symptom onset among two successive cases in a transmission chain [68].  
255 The infectiousness of a case is a function of the time since infection. This quantity is proportional to  $w_s$  if  
256 we set the timing of infection in the primary case as the time zero of  $w_s$  and assume that the generation  
257 interval equals the SI. The SI was assumed to follow a gamma distribution with a mean of 5.2 days and a  
258 standard deviation of 1.72 days [62]. Analytical estimates of  $R_t$  were obtained within a Bayesian  
259 framework using EpiEstim R package in R language [68].  $R_t$  was estimated at 7-day intervals. We  
260 reported the median and 95% credible interval (CrI).

261

### 262 **3. Results**

#### 263 **Case incidence data**

264 The Ministry of Health Chile reported a total of 481,342 COVID-19 cases as of November 2<sup>nd</sup>, 2020 [27].  
265 The epidemic curve showed an increasing trajectory from April-June 2020 and declined thereafter. On  
266 average, ~443 (SD: 133.6) new cases per day were reported in April 2020, ~2697 (SD:1342) new cases  
267 per day were reported in May 2020 and ~4943 (SD:972.2) new cases per day were reported in June 2020,  
268 the maximum number of cases reported per day during the epidemic. The per-day cases declined starting  
269 July, with ~2456 (SD:581) new cases reported per day in July 2020, ~1808 (SD:258) new cases per day  
270 reported in August 2020, ~1706 (SD:294) new cases per day reported in September 2020, and ~1521

271 (SD:275) new cases per day reported in October 2020. Figure 2 shows the daily incidence data of all  
272 confirmed cases in Chile as of November 2<sup>nd</sup>, 2020.

273

274 Figure 2: Daily incidence curve for all COVID-19 confirmed cases in Chile as of November 2<sup>nd</sup>, 2020 (9).

275

### 276 **Initial growth dynamics and estimate of the reproduction number using GGM**

277 We estimate the reproduction number for the first 27 epidemic days incorporating the effects of the social  
278 distancing interventions, as explained in Table 1 and Figure 1. The incidence curve displays sub-  
279 exponential growth dynamics with the scaling of growth parameter (deceleration of growth parameter),  $p$ ,  
280 estimated at 0.77 (95% CI: 0.73, 0.81) and the intrinsic growth rate,  $r$ , estimated at 0.81 (95% CI: 0.67,  
281 1.0). During the early transmission phase the reproduction number was estimated at 1.8 (95% CI: 1.6, 1.9)  
282 (Figure 3).

283

284 Figure 3 : Reproduction number with 95% CI estimated using the GGM model. The estimated  
285 reproduction number of the COVID-19 epidemic in Chile as of March 28<sup>th</sup>, 2020 is 1.8 (95% CI: 1.6, 1.9).

286

### 287 **Growth dynamics and estimate of reproduction number using GLM by July 7, 2020**

288 We also estimate the reproduction number from May 9<sup>th</sup>- July 7<sup>th</sup>, 2020, incorporating the effects of the  
289 reimplementations of localized lockdowns in Santiago, Antofagasta, and Valparaíso. The incidence curve  
290 displays a nearly linear growth trend with the deceleration of growth parameter,  $p$ , estimated at 0.51 (95%  
291 CI: 0.47, 0.56). The deceleration parameter in the GLM model helps modulate the trajectory of the  
292 epidemic, depicting a linear growth trend. The intrinsic growth rate,  $r$ , was estimated at 22 (95% CI: 13,  
293 31) and the final epidemic size,  $k_0$ , estimated at 3.4 e+05 (95% CI: 3.1 e+05, 3.7 e+05). The reproduction  
294 number was estimated at 0.87 (95% CI: 0.84, 0.89) as of July 7<sup>th</sup>, 2020 (Figure 4).

295

296 Figure 4: Reproduction number with 95% CI estimated by calibrating the GLM model from May 9<sup>th</sup>-July  
297 7<sup>th</sup>, 2020. The estimated reproduction number of the COVID-19 epidemic in Chile as of July 7<sup>th</sup>, 2020 is,  
298 0.87 (95% CI: 0.84, 0.89).

299

### 300 **Estimate of instantaneous reproduction number using Cori method**

301 Utilizing the Cori method based on a sliding weekly window, we observe that the reproduction number  
302 peaked on March 16<sup>th</sup>, 2020, with an estimate of  $R \sim 6.19$  (95% CrI= 5.84, 7.08). The reproduction  
303 number declined thereafter and reached  $\sim 1.00$  (95% CrI: 0.99, 1.04) on April 17<sup>th</sup>, 2020. From April 18<sup>th</sup>-  
304 June 18<sup>th</sup>, 2020 the reproduction number fluctuated between 1.01-1.75. This was followed by a decline in  
305 the reproduction number to less than 1.0 between June 19<sup>th</sup>-August 9<sup>th</sup>, 2020. Since then, the reproduction  
306 number has fluctuated around 1.0 with the most recent estimate of  $R \sim 0.96$  (95% CrI: 0.95, 0.98) (Figure  
307 5).

308

309 Figure 5: Estimate of instantaneous reproduction number ( $R$ ) for the COVID-19 epidemic in Chile as of  
310 November 2<sup>nd</sup>, 2020 using the Cori method. The most recent estimate of  $R \sim 0.96$  (95% CrI: 0.95, 0.98) as  
311 of November 2<sup>nd</sup>, 2020. Black solid line represents the mean  $R$  and the gray shaded region represents the  
312 95% credible interval around mean  $R$ .

313

### 314 **Assessing the impact of social distancing interventions**

315 To assess the impact of social distancing interventions in Chile given in Table 1, we generated a 20-day  
316 ahead forecast for Chile based on the daily incidence curve until March 30<sup>th</sup>, 2020. The 28-day calibration  
317 period of the GGM model yields an estimated growth rate,  $r$ , at 0.8 (95% CI: 0.6, 1.0) and a deceleration  
318 of growth parameter,  $p$ , at 0.8 (95% CI: 0.7, 0.8), indicating early sub-exponential growth dynamics. The  
319 20-day ahead forecast suggested that the early social distancing measures significantly slowed down the  
320 early spread of the virus in Chile, whose effect is noticeable about two weeks after implementing an  
321 intervention, as shown in Figure 6. A case resurgence was observed in Chile in mid-May 2020. As a

322 consequence of this case resurgence, a total lockdown was imposed in Greater Santiago (representing  
323 ~52% of total COVID-19 cases during the epidemic) on May 15<sup>th</sup>, 2020. The quarantine in Santiago was  
324 gradually eased from August 17, 2020, and was lifted on September 28, 2020, as a part of the move to  
325 phase three of a five-step plan of deconfinement that would allow movement on regional transportation  
326 and reopening of non-essential businesses and schools [31, 69, 70]. We generated a 20-day ahead forecast  
327 based on the daily incidence curve from May 9<sup>th</sup>-July 7<sup>th</sup>, 2020. The 60-day calibration of the GLM model  
328 yields an estimated scaling of the growth parameter,  $p$ , at 0.52 (95% CI: 0.47, 0.57), representing an  
329 almost linear growth pattern. The 20-day ahead average forecast utilizing the GLM model showed that  
330 Chile could accumulate ~45,160 cases (95% CI: 27,934-67,600) between July 8<sup>th</sup>-July 27<sup>th</sup>, 2020 (Figure  
331 7). Our forecast results approximate closely the ~46798 cases reported between July 8<sup>th</sup>-July 27<sup>th</sup>, 2020 by  
332 the Ministry of Health, Chile.

333  
334 Figure 6: 20-days ahead forecast of the COVID-19 epidemic in Chile by calibrating the GGM model until  
335 March 30<sup>th</sup>, 2020. Blue circles correspond to the data points; the solid red line indicates the best model fit,  
336 and the red dashed lines represent the 95% prediction interval. The vertical black dashed line represents  
337 the time of the start of the forecast period.

338  
339 Figure 7: 20-days ahead forecast of the COVID-19 epidemic in Chile by calibrating the GLM model from  
340 May 9<sup>th</sup>-July 7<sup>th</sup>, 2020. Blue circles correspond to the data points; the solid red line indicates the best  
341 model fit, and the red dashed lines represent the 95% prediction interval. The vertical black dashed line  
342 represents the time of the start of the forecast period.

343

#### 344 **COVID-19 Testing rates and positivity rate**

345 Daily testing and positivity rates for the time period April 9<sup>th</sup>-November 2<sup>nd</sup>, 2020, by the reporting date  
346 are shown in Figure 8. The total number of tests performed for this time period were 4,325,617, amongst  
347 which 10.9% (47,597) had positive results. The average number of daily tests was estimated at ~5,460 for



348 April 2020 and ~12,959 for May 2020, a 137% increase. The testing rate in Chile further increased in  
349 June 2020, testing on average ~17,578 individuals per day, followed by a slight decline in July 2020,  
350 testing on average 16587 individuals per day. However, the testing rates continued to increase in August  
351 (average ~26,079 tests per day), September (average ~29,663 tests per day), and October (average  
352 ~31,821 tests per day), indicating an expanding testing capacity of the country. The positivity rate  
353 (percentage of positive tests among the total number of tests) has fluctuated from a monthly average of  
354 ~9.07% (SD: 2.3) in April 2020 to a monthly average of ~4.87% (SD: 0.65) in October 2020.

355

356 Figure 8: Laboratory results for the COVID-19 tests conducted in Chile as of November 2<sup>nd</sup>, 2020. The  
357 blue color represents the negative test results, and the yellow color represents the positive test results. The  
358 solid orange line represents the positivity rate of COVID-19 in Chile.

359

#### 360 **4. Discussion**

361 The estimates of the early transmission potential in Chile for the first 27 days of the epidemic indicate  
362 sustained local transmission in the country with the estimate of reproduction number  $R$  at ~1.8 (95% CI:  
363 1.6, 1.9) which is also in accordance with the estimate of the reproduction number obtained from the Cori  
364 method ( $R \sim 2.2$  95% CrI (2.14, 2.28)). The estimates of  $R$  from our analysis agree with the estimates of  $R$   
365 retrieved from studies conducted in the surrounding Latin American countries including Peru and Brazil  
366 [71, 72]. Other countries including Korea, South Africa and Iran also exhibit similar estimates of  $R$  that  
367 lie in the range of 1.5-7.1 [73-80]. In contrast, some other countries including Singapore and Australia  
368 have reported much lower estimates of  $R$  ( $R < 1$ ) that can be correlated with the implementation of early  
369 strict social distancing interventions in these countries [81, 82].

370

371 The initial deceleration of the growth parameter in Chile indicates a sub-exponential growth pattern  
372 ( $p \sim 0.8$ ), consistent with sub-exponential growth patterns of COVID-19 that have been observed in

373 Singapore ( $p \sim 0.7$ ), Korea ( $p \sim 0.76$ ) and other Chinese provinces excluding Hubei ( $p \sim 0.67$ ) [78, 81, 83].  
374 In contrast, studies conducted in Peru, a Latin American country, and Iran have reported a nearly  
375 exponential growth pattern of the COVID-19 whereas an exponential growth pattern has been reported in  
376 China [72, 75, 83].

377

378 Although the initial transmission stage of COVID-19 in Chile has been attributed to multiple case  
379 importations, Chile quickly implemented control measures against the COVID-19 epidemic, including  
380 border closures on March 18<sup>th</sup>, 2020, to prevent further case importations. The 20-day ahead forecast of  
381 our GGM model calibrated to 28 days suggest that the social distancing measures, including closure of  
382 schools, universities and day cares, have helped slow down the early virus spread in the country by  
383 reducing population mobility (Table 1, Figure 1, Figure 6) [84]. The commixture of interventions,  
384 including localized lockdowns, night-time curfew, school closures, and the ban on social gatherings in  
385 Chile, can probably be attributed to preventing the disease trend from growing exponentially during the  
386 early growth phase, as has occurred elsewhere [3, 4]. However, the significant increase in case incidence  
387 observed in mid-May can probably be attributed to the relaxation of social distancing measures and  
388 reopening of society in late April, in the context of the “Safe Return” plan [31]. As the virus reached the  
389 lower-income neighborhoods in Chile, the pandemic quickly exploded [23, 38, 39, 85]. While the  
390 COVID-19 case incidence exhibited a relative stabilization in case trajectory for April 2020 (with an  
391 average of ~443 cases per day), highlighting the positive effects of early quarantine and lockdowns, the  
392 reopening of society and early economic reactivation in late April 2020 probably resulted in the surge of  
393 cases resulting in an acceleration of the epidemic with estimates of  $R$  higher than 1.0. The total lockdown  
394 comprised of stay-at-home orders imposed in Greater Santiago (which accounted for about 77% of cases  
395 in the country) on May 15<sup>th</sup> showed an effect in slowing the virus's transmission. Similar lockdowns were  
396 imposed in Antofagasta on May 5<sup>th</sup> and in Valparaíso on June 12<sup>th</sup>, though these regions together  
397 represent only ~10% of cases in Chile [31]. The deceleration of growth parameter,  $p$ , has been estimated

398 at  $\sim 0.51$  (95% CI: 0.47, 0.56) after the reimposition of lockdowns and social distancing measures in May,  
399 consistent with a linear incidence growth trend, indicating deceleration of the epidemic.

400

401 Moreover, we estimated a reproduction number,  $R$ , of  $\sim 0.87$  (95% CI: 0.84, 0.89) in early July, indicating  
402 a decline in transmission of the virus consistent with the stay-at-home orders. This reproduction number  
403 corresponds to the instantaneous reproduction number estimated during the course of the epidemic  
404 utilizing the Cori method, which also indicates a decrease in disease transmission with  $R \sim 0.8$  as of early  
405 July. The instantaneous reproduction number has fluctuated around  $\sim 1$  since early August with the most  
406 recent estimate of reproduction number,  $R \sim 0.9$  as of November 2<sup>nd</sup>, 2020. The 20-day ahead forecast  
407 calibrating data to the GLM model (from May 9<sup>th</sup>-July 7<sup>th</sup>, 2020) has reasonably indicated a declining  
408 trend in case incidence. The forecast results also imply that approximately  $\sim 45,160$  cases (95% CI:  
409 27,934-67,600) could be observed in Chile from July 8<sup>th</sup>-July 27<sup>th</sup>, 2020. The actual case count by for this  
410 time period, as reported by the Chilean government indicated 46,798 cases, closely approximating our  
411 mean GLM forecast, falling within the 95% PI. Therefore, based on the most recent estimates of  $R$   
412 (Figure 5), it can be implied that maintaining social distancing measures, limiting social gatherings, and  
413 reducing population mobility have served as essential ways to containing the spread of the virus [86, 87].

414

415 Though the number of reported cases in Latin America remains low compared to the United States,  
416 official data for many Latin American countries are incomplete. However, Chile has tested a higher  
417 percentage of its residents than any other Latin American nation, lending confidence to its reliability [88].  
418 Chile's testing capabilities have been greatly expanded during the pandemic, in part from a coordinated  
419 effort lead by the Ministry of Science to include testing from public and private laboratories. For instance,  
420 the average number of COVID-19 tests performed in Chile per day per thousand people is 1.52 compared  
421 to the neighboring South American country, Peru ( $\sim 0.2$  tests per thousand people) [89]. The average  
422 positivity rate for the whole span of the epidemic in Chile is estimated at  $\sim 12.98\%$ . However, the average  
423 monthly positivity rate of COVID-19 in Chile is estimated at  $\sim 5.90\%$  and  $\sim 4.88\%$  for September and

424 October, respectively, compared to ~20.09% in May 2020. The high positivity rate at the beginning of the  
425 epidemic indicates that the government failed to cast a wide enough net to test the masses early in the  
426 pandemic, and there were probably many more active cases than those detected by epidemiological  
427 surveillance, underestimating the epidemic growth curve [90-92]. The most recent lower testing rates  
428 indicate that Chile is testing a comparatively larger segment of the population. This positivity rate for  
429 Chile is also consistent with the positivity rate obtained from India, the United States, Canada, and  
430 Germany that exhibit moderately high positivity rates (4-8%) for COVID-19, indicating overall limited  
431 testing in these countries [89, 93]. In comparison, some countries like Mexico and the Czech Republic  
432 exhibit very high positivity rates (30-51%) [89]. Other countries like Denmark, New Zealand, Australia,  
433 Singapore, and South Korea have reached very low positivity rates (0-3%) by testing the masses with  
434 South Korea's large testing capacity combined with a strategy that tracks infected people via cell phones  
435 [88, 89, 94]. Moreover, studies suggest there is asymptomatic transmission of SARS-CoV-2 [66, 95, 96],  
436 which means we could have underestimated our estimates based on the daily incidence's growth trend  
437 from symptomatic cases [97-99]. On the other hand, preliminary results of a study have shown the  
438 relative transmission of asymptomatic cases in Santiago to be almost ~3% [100]. While our study  
439 highlights the effectiveness of broad-scale social distancing and control interventions in Chile, it also  
440 underscores the need for persistent isolation and social distancing measures to stomp all active disease  
441 transmission chains in Chile. In the absence of pharmacological interventions and considering the advent  
442 of second waves in Asia and Europe, non-pharmacological interventions such as the ones implemented in  
443 Chile are the available options for countries to address the pandemic before large segments of the  
444 population are immunized with effective and safe vaccines. In this scenario, real-time metrics that  
445 characterize the transmission dynamics and control are crucial to face the future challenges that the  
446 pandemic will impose.

447

448 This study has some limitations. First, our study analyzes cases by the dates of reporting while it is ideal  
449 to analyze the cases by the dates of onset or after adjusting for reporting delays. On the other hand, a

450 substantial fraction of the COVID-19 infections exhibits very mild or no symptoms at all, which may not  
451 be reflected by data [101, 102]. Moreover, the data are not stratified by local and imported cases;  
452 therefore, we assumed that all cases contribute equally to the transmission dynamics of COVID-19.  
453 Finally, the extent of selective underreporting, and its impact on these results is difficult to assess.

454

## 455 **5. Conclusions**

456 In this study, we estimate the transmission potential of SARS-CoV-2 in Chile. Our current findings point  
457 to sustained transmission of SARS-CoV-2 in the early phase of the outbreak, with our estimate of the  
458 reproduction number at  $R \sim 1.8$ . The COVID-19 epidemic in Chile followed an early sub-exponential  
459 growth trend ( $p \sim 0.8$ ) which has transformed into an almost linear growth trend ( $p \sim 0.5$ ) as of July 7<sup>th</sup>,  
460 2020. The most recent estimate of reproduction number,  $R$ , is  $\sim 0.9$  as of November 2<sup>nd</sup>, 2020, indicating a  
461 decline in the virus transmission in Chile. The implementation of lockdowns and apt social distancing  
462 interventions have indeed slowed the spread of the virus. However, the number of new COVID-19 cases  
463 continue to accumulate, underscoring the need for persistent social distancing and active contact tracing  
464 efforts to maintain the epidemic under control.

465

466 **Author Contributions:** Conceptualization, G.C. and A.T.; methodology, G.C, A.T.; validation, G.C.;  
467 formal analysis, A.T., G.C.; investigation, A.T.; resources, G.C., A.T.; data curation, A.T.; writing—  
468 original draft preparation, A.T., G.C.; writing, review and editing, A.T., G.C., E.U, C.C, K.V., R.R, R.L,  
469 G.C.; visualization, A.T., G.C.; supervision, G.C.; project administration, G.C.; funding acquisition, G.C.  
470 All authors have read and agreed to the published version of the manuscript.

471

472 **Funding:** G.C. is partially supported from NSF grants 1610429 and 1633381 and R01 GM 130900. EU is  
473 partially funded by the ANID Millennium Science Initiative [grant NCN17\_081]

474

## 475 **Availability of data and materials**

476 The datasets used and analyzed during the current study are available from Base de Datos COVID-19  
477 repository, <http://www.minciencia.gob.cl/covid19>.

478

479 **Conflicts of Interest:** The authors declare no conflict of interest.

480

## 481 **References**

- 482 1. WHO. WHO Director-General's opening remarks at the media briefing on COVID-19-11 March 2020 World  
483 Health Organization2020 [April 23]. Available from: <https://bit.ly/2A8aC1Q>.
- 484 2. Chan JF-W, Yuan S, Kok K-H, To KK-W, Chu H, Yang J, et al. A familial cluster of pneumonia associated  
485 with the 2019 novel coronavirus indicating person-to-person transmission: a study of a family cluster. *The Lancet*.  
486 2020;395(10223):514-23. doi: 10.1016/S0140-6736(20)30154-9.
- 487 3. Li Y, Campbell H, Kulkarni D, Harpur A, Nundy M, Wang X, et al. The temporal association of introducing  
488 and lifting non-pharmaceutical interventions with the time-varying reproduction number (R) of SARS-CoV-2: a  
489 modelling study across 131 countries. *The Lancet Infectious Diseases*. 2020. Epub October 22. doi: 10.1016/S1473-  
490 3099(20)30785-4.
- 491 4. Walker PGT, Whittaker C, Watson OJ, Baguelin M, Winskill P, Hamlet A, et al. The impact of COVID-19 and  
492 strategies for mitigation and suppression in low- and middle-income countries. *Science (New York, NY)*.  
493 2020;369(6502):413-22. doi: 10.1126/science.abc0035.
- 494 5. Flaxman S, Mishra S, Gandy A, Unwin HJT, Mellan TA, Coupland H, et al. Estimating the effects of non-  
495 pharmaceutical interventions on COVID-19 in Europe. *Nature*. 2020;584(7820):257-61. doi: 10.1038/s41586-020-2405-7.
- 496 6. Dong E, Du H, Gardner L. An interactive web-based dashboard to track COVID-19 in real time. *The Lancet*  
497 *Infectious Diseases*. 2020;20(5):533-4. doi: 10.1016/S1473-3099(20)30120-1.
- 498 7. Bank W. The Economy in the Time of Covid-19. LAC Semiannual Report. Washington, DC: World Bank:  
499 2020 April 12. Report No.
- 500 8. Baek C, Mccrory PB, Messer T, Mui P. Unemployment effects of stay-at-home orders: Evidence from high  
501 frequency claims data. *The Review of Economics and Statistics*. 2020:1-72.
- 502 9. Rojas FL, Jiang X, Montenegro L, Simon KI, Weinberg BA, Wing C. Is the Cure Worse than the Problem  
503 Itself? Immediate Labor Market Effects of COVID-19 Case Rates and School Closures in the U.S. National Bureau of  
504 Economic Research. 2020;(0898-2937). doi: 10.3386/w27127.
- 505 10. Gupta S, Montenegro L, Nguyen TD, Rojas FL, Schmutte IM, Simon KI, et al. Effects of Social Distancing  
506 Policy on Labor Market Outcomes. National Bureau of Economic Research Working Paper Series. 2020;No. 27280.  
507 doi: 10.3386/w27280.
- 508 11. Pfefferbaum B, North CS. Mental Health and the Covid-19 Pandemic. *New England Journal of Medicine*.  
509 2020;383(6):510-2. doi: 10.1056/NEJMp2008017. PubMed PMID: 32283003.
- 510 12. De Girolamo G, Cerveri G, Clerici M, Monzani E, Spinogatti F, Starace F, et al. Mental Health in the  
511 Coronavirus Disease 2019 Emergency—The Italian Response. *JAMA Psychiatry*. 2020;77(9):974-6. doi:  
512 10.1001/jamapsychiatry.2020.1276.
- 513 13. Asahi K, Undurraga EA, Valdes R, Wagner R. The effect of COVID-19 on the economy: evidence from an  
514 early adopter of localized lockdowns. medRxiv. 2020:2020.09.21.20198887. doi: 10.1101/2020.09.21.20198887.
- 515 14. Okada P, Buathong R, Phuygun S, Thanadachakul T, Parnmen S, Wongboot W, et al. Early transmission  
516 patterns of coronavirus disease 2019 (COVID-19) in travellers from Wuhan to Thailand, January 2020. *Euro*  
517 *surveillance* : bulletin Europeen sur les maladies transmissibles = European communicable disease bulletin.

- 518 2020;25(8). Epub 2020/03/05. doi: 10.2807/1560-7917.Es.2020.25.8.2000097. PubMed PMID: 32127124; PubMed Central  
519 PMCID: PMC7055038.
- 520 15. Spiteri G, Fielding J, Diercke M, Campese C, Enouf V, Gaymard A, et al. First cases of coronavirus disease  
521 2019 (COVID-19) in the WHO European Region, 24 January to 21 February 2020. Euro surveillance  
522 2020;25(9):2000178. doi: 10.2807/1560-7917.ES.2020.25.9.2000178. PubMed PMID: 32156327.
- 523 16. Holshue ML, DeBolt C, Lindquist S, Lofy KH, Wiesman J, Bruce H, et al. First Case of 2019 Novel  
524 Coronavirus in the United States. New England Journal of Medicine. 2020;382(10):929-36. doi:  
525 10.1056/NEJMoa2001191.
- 526 17. WHO. Situation Reports Coronavirus World Health Organization2020 [March 5]. Available from:  
527 <https://www.who.int/emergencies/diseases/novel-coronavirus-2019/situation-reports>.
- 528 18. Taylor L. How South America became the new centre of the coronavirus pandemic. NewScientist. 2020 June  
529 10.
- 530 19. COVID-19 in Latin America: a humanitarian crisis. The Lancet. 2020;396(10261):1463. doi: 10.1016/S0140-  
531 6736(20)32328-X.
- 532 20. Undurraga EA, Chowell G, Mizumoto K. Case fatality risk by age from COVID-19 in a high testing setting  
533 in Latin America: Chile, March-May, 2020. Infectious Disease Poverty. 2020;(In press).
- 534 21. Munayco C, Chowell G, Tariq A, Undurraga EA, Mizumoto K. Risk of death by age and gender from  
535 CoVID-19 in Peru, March-May, 2020. Aging (Albany NY). 2020;12(14):13869-81. Epub 2020/07/21. doi:  
536 10.18632/aging.103687. PubMed PMID: 32692724.
- 537 22. Taylor L. How Latin America is fighting covid-19, for better and worse. BMJ. 2020;370:m3319. doi:  
538 10.1136/bmj.m3319.
- 539 23. Gil M, Undurraga E. CoVID-19 has exposed how 'the other half' (still) lives. Bulletin of Latin American  
540 Research. 2020;In press.
- 541 24. De Souza WM, Buss LF, Candido DdS, Carrera J-P, Li S, Zarebski AE, et al. Epidemiological and clinical  
542 characteristics of the COVID-19 epidemic in Brazil. Nature Human Behaviour. 2020;4(8):856-65. doi: 10.1038/s41562-  
543 020-0928-4.
- 544 25. Garcia PJ, Alarcón A, Bayer A, Buss P, Guerra G, Ribeiro H, et al. COVID-19 Response in Latin America. The  
545 American Journal of Tropical Medicine and Hygiene. 2020;103(5):1765-72. doi: <https://doi.org/10.4269/ajtmh.20-0765>.
- 546 26. González-Bustamante B. Evolution and early government responses to COVID-19 in South America. World  
547 Development. 2021;137:105180. doi: <https://doi.org/10.1016/j.worlddev.2020.105180>.
- 548 27. Government of Chile M. MinScience/ Data-COVID19  
549 2020 [cited 2020 April 25]. Available from: <https://github.com/MinCiencia/Datos-COVID19>.
- 550 28. MOH. Cifras Oficiales COVID-19 2020. Available from: <https://www.gob.cl/coronavirus/cifrasoficiales/>.
- 551 29. Chile Gd. Chile enters the Stage 4 Coronavirus transmission scenario and President Piñera announces the  
552 closure of the borders and secures the supply chain. Gob.cl: 2020 March 16. Report No.
- 553 30. Cambero F. Chile bans large public events over coronavirus fears, ahead of planned protests. Reuters. 2020  
554 March 13.
- 555 31. (MINSAL) MdS. Plan de acción por coronavirus 2020 [cited 2020 July 1]. Available from:  
556 <https://www.gob.cl/coronavirus/plandeaccion/>.
- 557 32. MOH. Dispone medidas sanitarias que indica por brote de COVID-19.Norms 1143498, 1143591, 1746958,  
558 1143651,1143645 Biblioteca del Congreso Nacional de Chile2020 [April 24]. Available from:  
559 <https://www.leychile.cl/N?:i=1143498&f=2020-04-04&p=>.
- 560 33. Wires N. Chile's capital goes into strict lockdown after Covid-19 surge. France 24. 2020 May 17.
- 561 34. Prensa Presidencia GC. "Presidente Piñera presenta Plan Retorno Seguro: "Hoy es tiempo de poner a Chile  
562 por delante"." 2020 [cited 2020 June 10]. Available from: <https://prensa.presidencia.cl/comunicado.aspx?id=150453>.
- 563 35. Tercera L. 55% of the stores open and lines to enter: This was the reopening of the Mall Apumanque under  
564 strict protocol. La Tercera. 2020 April 30.
- 565 36. Li Y, Undurraga EA, Zubizarreta JR. Effectiveness of Localized Lockdowns in the SARS-CoV-2 Pandemic.  
566 medRxiv. 2020:2020.08.25.20182071. doi: 10.1101/2020.08.25.20182071.
- 567 37. Beaubien J. How Chile Ended Up With One Of The Highest COVID-19 Rates. npr. 2020 July 2.
- 568 38. Bennett M. All things equal? Heterogeneity in policy effectiveness against COVID-19 spread in Chile. World  
569 development. 2021;137:105208-. Epub 2020/09/24. doi: 10.1016/j.worlddev.2020.105208. PubMed PMID: 32994662.

- 570 39. Canals M, Cuadrado C, Canals A, Yohannessen K, Lefio LA, Bertoglia MP, et al. Epidemic trends, public  
571 health response and health system capacity: the Chilean experience in four months of the COVID-19 pandemic. *Rev*  
572 *Panam Salud Publica*. 2020;44:e99-e. doi: 10.26633/RPSP.2020.99. PubMed PMID: 32821259.
- 573 40. Gob.cl. Official figures COVID-19 2020 [cited 2020 April 24]. Available from:  
574 <https://www.gob.cl/coronavirus/cifrasoficiales/#reportes>.
- 575 41. Government of Chile M. COVID-19 data. Github2020.
- 576 42. MOH. Cifras Oficiales COVID-19, Ministry of Health, Plan de Acción Coronavirus COVID-19 2020 [April  
577 2]. Available from: <https://www.gob.cl/coronavirus/cifrasoficiales/>.
- 578 43. Nishiura H, Chowell G. Early transmission dynamics of Ebola virus disease (EVD), West Africa, March to  
579 August 2014. *Euro surveillance : bulletin Europeen sur les maladies transmissibles = European communicable disease*  
580 *bulletin*. 2014;19(36). Epub 2014/09/19. PubMed PMID: 25232919.
- 581 44. Nishiura H, Chowell G. The Effective Reproduction Number as a Prelude to Statistical Estimation of Time-  
582 Dependent Epidemic Trends. Springer, editor2009. 103-12 p.
- 583 45. Shanafelt DW, Jones G, Lima M, Perrings C, Chowell G. Forecasting the 2001 Foot-and-Mouth Disease  
584 Epidemic in the UK. *Ecohealth*. 2018;15(2):338-47. Epub 2017/12/13. doi: 10.1007/s10393-017-1293-2. PubMed PMID:  
585 29238900.
- 586 46. Roosa K, Lee Y, Luo R, Kirpich A, Rothenberg R, Hyman JM, et al. Short-term Forecasts of the COVID-19  
587 Epidemic in Guangdong and Zhejiang, China: February 13-23, 2020. *Journal of clinical medicine*. 2020;9(2):596. doi:  
588 10.3390/jcm9020596. PubMed PMID: 32098289.
- 589 47. Chowell G, Hincapie-Palacio D, Ospina J, Pell B, Tariq A, Dahal S, et al. Using Phenomenological Models to  
590 Characterize Transmissibility and Forecast Patterns and Final Burden of Zika Epidemics. *Public Library of Science*  
591 *Currents*. 2016;8:ecurrents.outbreaks.f14b2217c902f453d9320a43a35b583. doi:  
592 10.1371/currents.outbreaks.f14b2217c902f453d9320a43a35b583. PubMed PMID: 27366586.
- 593 48. Pública MdlyS. Declares status of constitutional exception of catastrophe, by public calamity, in the territory  
594 of Chile Biblioteca del Congreso Nacional de Chile. 2020 [April 22]. Available from:  
595 <https://www.leychile.cl/Navegar?idNorma=1143580&idVersion=2020-03-26&idParte=>.
- 596 49. Regan H, Yeung J, Renton A, Woodyatt A, Meg Wagner. Chile mandates face masks on public and private  
597 transportation. *CNN*. 2020 April 6.
- 598 50. Mostrado E. Among applause: Mayor Lavín launches pilot plan to open the Apumanque mall. *elm* strador.  
599 2020 April30.
- 600 51. Chile A. Total quarantine in Santiago: what time, when does it start and until what day does it extend.  
601 *Tikitakas*. 2020 May 15.
- 602 52. Chowell G, Tariq A, Hyman JM. A novel sub-epidemic modeling framework for short-term forecasting  
603 epidemic waves. *BioMed Central Medicine*. 2019;17(1):164. doi: 10.1186/s12916-019-1406-6.
- 604 53. Pell B, Kuang Y, Viboud C, Chowell G. Using phenomenological models for forecasting the 2015 Ebola  
605 challenge. *Epidemics*. 2018;22:62-70. Epub 2016/12/04. doi: 10.1016/j.epidem.2016.11.002. PubMed PMID: 27913131.
- 606 54. Chowell G. Fitting dynamic models to epidemic outbreaks with quantified uncertainty: A primer for  
607 parameter uncertainty, identifiability, and forecasts. *Infectious Disease Modelling*. 2017;2(3):379-98. doi:  
608 <https://doi.org/10.1016/j.idm.2017.08.001>.
- 609 55. Viboud C, Simonsen L, Chowell G. A generalized-growth model to characterize the early ascending phase  
610 of infectious disease outbreaks. *Epidemics*. 2016;15:27-37. doi: <https://doi.org/10.1016/j.epidem.2016.01.002>.
- 611 56. Chowell G, Sattenspiel L, Bansal S, Viboud C. Mathematical models to characterize early epidemic growth:  
612 A review. *Physics of Life Reviews*. 2016;18:66-97. doi: <https://doi.org/10.1016/j.plrev.2016.07.005>.
- 613 57. Chowell G, Luo R, Sun K, Roosa K, Tariq A, Viboud C. Real-time forecasting of epidemic trajectories using  
614 computational dynamic ensembles. *Epidemics*. 2020;30:100379. doi: <https://doi.org/10.1016/j.epidem.2019.100379>.
- 615 58. Chowell G, Ammon CE, Hengartner NW, Hyman JM. Transmission dynamics of the great influenza  
616 pandemic of 1918 in Geneva, Switzerland: Assessing the effects of hypothetical interventions. *Journal of Theoretical*  
617 *Biology*. 2006;241(2):193-204. doi: <https://doi.org/10.1016/j.jtbi.2005.11.026>.
- 618 59. Chowell G, Abdirizak F, Lee S, Lee J, Jung E, Nishiura H, et al. Transmission characteristics of MERS and  
619 SARS in the healthcare setting: a comparative study. *BioMed Central Medicine*. 2015;13(1):210. doi: 10.1186/s12916-  
620 015-0450-0.
- 621 60. Anderson RM, May RM. *Infectious Diseases of Humans*. Oxford, editor. Oxford Univeristy Press1991.

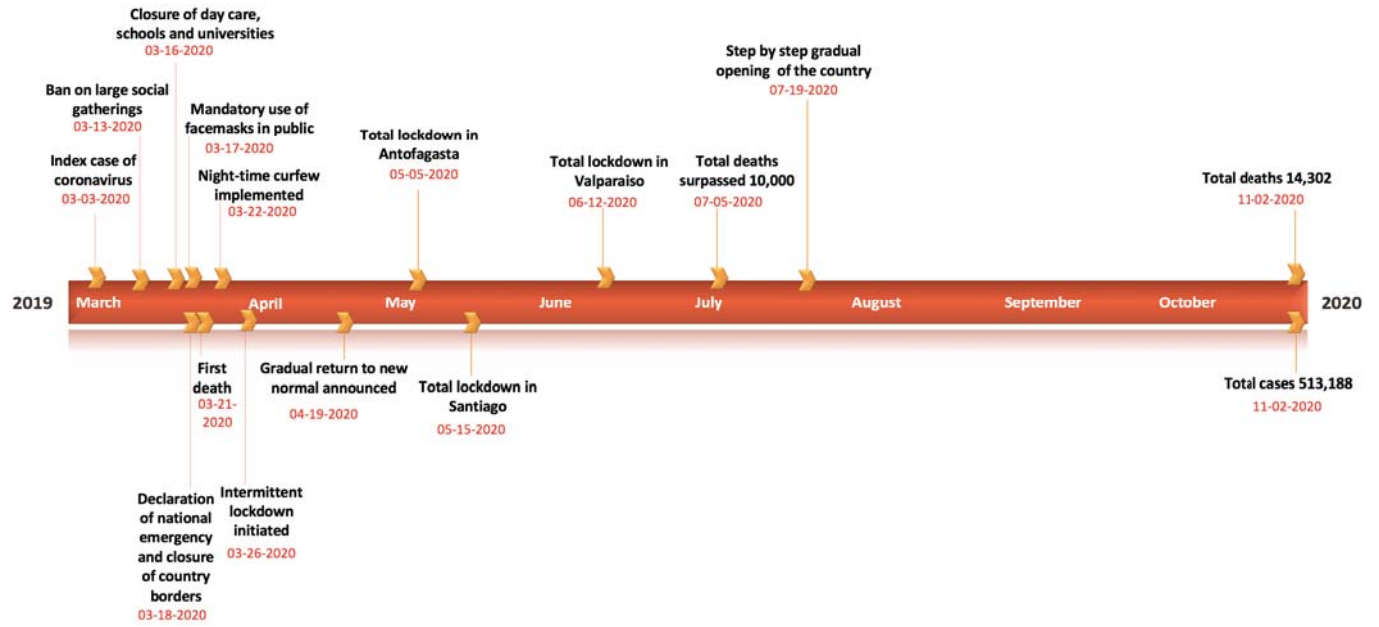


- 622 61. Nishiura H, Chowell G, Heesterbeek H, Wallinga J. The ideal reporting interval for an epidemic to  
623 objectively interpret the epidemiological time course. *J R Soc Interface*. 2010;7(43):297-307. Epub 2009/07/01. doi:  
624 10.1098/rsif.2009.0153. PubMed PMID: 19570792.
- 625 62. Ganyani T, Kremer C, Chen D, Torneri A, Faes C, Wallinga J, et al. Estimating the generation interval for  
626 coronavirus disease (COVID-19) based on symptom onset data, March 2020. *Eurosurveillance*. 2020;25(17):2000257.  
627 doi: doi:<https://doi.org/10.2807/1560-7917.ES.2020.25.17.2000257>.
- 628 63. Paine S, Mercer G, Kelly P, Bandaranayake D, Baker M, Huang Q, et al. Transmissibility of 2009 pandemic  
629 influenza A(H1N1) in New Zealand: effective reproduction number and influence of age, ethnicity and importations.  
630 *Euro surveillance : bulletin European sur les maladies transmissibles = European communicable disease bulletin*.  
631 2010;15(24). Epub 2010/06/26. PubMed PMID: 20576236.
- 632 64. Fraser C. Estimating Individual and Household Reproduction Numbers in an Emerging Epidemic. *PLOS*  
633 *ONE*. 2007;2(8):e758. doi: 10.1371/journal.pone.0000758.
- 634 65. Chong KC, Zee BCY, Wang MH. Approximate Bayesian algorithm to estimate the basic reproduction  
635 number in an influenza pandemic using arrival times of imported cases. *Travel medicine and infectious disease*.  
636 2018;23:80-6. Epub 2018/04/14. doi: 10.1016/j.tmaid.2018.04.004. PubMed PMID: 29653203.
- 637 66. He X, Lau EHY, Wu P, Deng X, Wang J, Hao X, et al. Temporal dynamics in viral shedding and  
638 transmissibility of COVID-19. *Nature Medicine*. 2020;26(5):672-5. doi: 10.1038/s41591-020-0869-5.
- 639 67. Wallinga J, Teunis P. Different Epidemic Curves for Severe Acute Respiratory Syndrome Reveal Similar  
640 Impacts of Control Measures. *American Journal of Epidemiology*. 2004;160(6):509-16. doi: 10.1093/aje/kwh255.
- 641 68. Cori A, Ferguson NM, Fraser C, Cauchemez S. A New Framework and Software to Estimate Time-Varying  
642 Reproduction Numbers During Epidemics. *American Journal of Epidemiology*. 2013;178(9):1505-12. doi:  
643 10.1093/aje/kwt133.
- 644 69. Gardaworld. Chile: Authorities lift COVID-19 lockdown measures in Santiago from September 28 /update  
645 34 Gardaworld2020 [cited 2020 November 2]. Available from: [https://www.garda.com/crisis24/news-  
646 alerts/384111/chile-authorities-lift-covid-19-lockdown-measures-in-santiago-from-september-28-update-34](https://www.garda.com/crisis24/news-alerts/384111/chile-authorities-lift-covid-19-lockdown-measures-in-santiago-from-september-28-update-34).
- 647 70. Gradaworld. Chile: Authorities to gradually lift lockdown restrictions in central Santiago from August 17  
648 /update 24 Gradaworld2020 [cited 2020 November 2]. Available from: [https://www.garda.com/crisis24/news-  
649 alerts/368666/chile-authorities-to-gradually-lift-lockdown-restrictions-in-central-santiago-from-august-17-update-24](https://www.garda.com/crisis24/news-alerts/368666/chile-authorities-to-gradually-lift-lockdown-restrictions-in-central-santiago-from-august-17-update-24).
- 650 71. Felix FHC, Fontenele JB. Instantaneous R calculation for COVID-19 epidemic in Brazil. *medRxiv*.  
651 2020:2020.04.23.20077172. doi: 10.1101/2020.04.23.20077172.
- 652 72. Munayco CV, Tariq A, Rothenberg R, Soto-Cabezas GG, Reyes MF, Valle A, et al. Early transmission  
653 dynamics of COVID-19 in a southern hemisphere setting: Lima-Peru: February 29th–March 30th, 2020. *Infectious*  
654 *Disease Modelling*. 2020. doi: <https://doi.org/10.1016/j.idm.2020.05.001>.
- 655 73. Read JM, Bridgen JR, Cummings DA, Ho A, Jewell CP. Novel coronavirus 2019-nCoV: early estimation of  
656 epidemiological parameters and epidemic predictions. *medRxiv*. 2020:2020.01.23.20018549. doi:  
657 10.1101/2020.01.23.20018549.
- 658 74. Wu JT, Leung K, Leung GM. Nowcasting and forecasting the potential domestic and international spread of  
659 the 2019-nCoV outbreak originating in Wuhan, China: a modelling study. *The Lancet*. 2020;395(10225):689-97. doi:  
660 10.1016/S0140-6736(20)30260-9.
- 661 75. Muniz-Rodriguez K, Fung IC-H, Ferdosi SR, Ofori SK, Lee Y, Tariq A, et al. Transmission potential of  
662 COVID-19 in Iran. *medRxiv*. 2020:2020.03.08.20030643. doi: 10.1101/2020.03.08.20030643.
- 663 76. Mizumoto K, Kagaya K, Chowell G. Early epidemiological assessment of the transmission potential and  
664 virulence of coronavirus disease 2019 (COVID-19) in Wuhan City: China, January-February, 2020. *medRxiv*.  
665 2020:2020.02.12.20022434. doi: 10.1101/2020.02.12.20022434.
- 666 77. Hwang J, Park H, Kim S-H, Jung J, Kim N. Basic and effective reproduction numbers of COVID-19 cases in  
667 South Korea excluding Sincheonji cases. *medRxiv*. 2020:2020.03.19.20039347. doi: 10.1101/2020.03.19.20039347.
- 668 78. Shim E, Tariq A, Choi W, Lee Y, Chowell G. Transmission potential and severity of COVID-19 in South  
669 Korea. *International Journal of Infectious Diseases*. 2020;93:339-44. doi: 10.1016/j.ijid.2020.03.031.
- 670 79. Mbuva R, Marwala T. Bayesian Inference of COVID-19 Spreading Rates in South Africa. *medRxiv*.  
671 2020:2020.04.28.20083873. doi: 10.1101/2020.04.28.20083873.
- 672 80. Masjedi H, Rabajante JF, Bahrnizadd F, Zare MH. Nowcasting and Forecasting the Spread of COVID-19 in  
673 Iran. *medRxiv*. 2020:2020.04.22.20076281. doi: 10.1101/2020.04.22.20076281.

- 674 81. Tariq A, Lee Y, Roosa K, Blumberg S, Yan P, Ma S, et al. Real-time monitoring the transmission potential of  
675 COVID-19 in Singapore, March 2020. medRxiv. 2020:2020.02.21.20026435. doi: 10.1101/2020.02.21.20026435.
- 676 82. Price DJ, Shearer FM, Meehan MT, McBryde E, Moss R, Golding N, et al. Early analysis of the Australian  
677 COVID-19 epidemic. medRxiv. 2020:2020.04.25.20080127. doi: 10.1101/2020.04.25.20080127.
- 678 83. Roosa K, Lee Y, Luo R, Kirpich A, Rothenberg R, Hyman JM, et al. Real-time forecasts of the COVID-19  
679 epidemic in China from February 5th to February 24th, 2020. Infectious Disease Modelling. 2020;5:256-63. doi:  
680 <https://doi.org/10.1016/j.idm.2020.02.002>.
- 681 84. Cuadrado C, Monsalves MJ, Gajardo J, Bertoglia MP, Najera M, Alfaro T, et al. Impact of small-area  
682 lockdowns for the control of the COVID-19 pandemic. medRxiv. 2020:2020.05.05.20092106. doi:  
683 10.1101/2020.05.05.20092106.
- 684 85. Contesse J. Responding to COVID-19 Without Public Trust. The Regulatory Review. 2020 June 2.
- 685 86. France-Press A. Chile prolongs Santiago lockdown as daily virus deaths rise. The Jakarta Post. 2020 June 4.
- 686 87. Chang S, Pierson E, Koh PW, Gerardin J, Redbird B, Grusky D, et al. Mobility network models of COVID-19  
687 explain inequities and inform reopening. Nature. 2020. doi: 10.1038/s41586-020-2923-3.
- 688 88. Thomson E, Sanders P. Chile Charts New Path With Rolling Lockdowns, Immunity Cards. Bloomberg. 2020  
689 April 22.
- 690 89. Oxford Uo. Our World in Data: Oxford Martin School; 2020 [cited 2020 June 28]. Available from:  
691 <https://ourworldindata.org/coronavirus/country/peru?country=~PER#how-many-tests-are-performed-each-day>.
- 692 90. Li R, Pei S, Chen B, Song Y, Zhang T, Yang W, et al. Substantial undocumented infection facilitates the rapid  
693 dissemination of novel coronavirus (SARS-CoV-2). Science (New York, NY). 2020;368(6490):489-93. Epub 2020/03/18.  
694 doi: 10.1126/science.abb3221. PubMed PMID: 32179701; PubMed Central PMCID: PMCPCMC7164387.
- 695 91. Bhatia S, Imai N, Cuomo-Dannenburg G, Baguelin M, Boonyasiri A, Cori A, et al. Report 6: Relative  
696 sensitivity of international surveillance. Imperial College London COVID-19 Response Team: 2020 February 21.  
697 Report No.
- 698 92. Asahi K, Undurraga EA, Wagner R. Benchmarking the CoVID-19 pandemic across countries and states in  
699 the U.S.A. under heterogeneous testing. medRxiv. 2020:2020.05.01.20087882. doi: 10.1101/2020.05.01.20087882.
- 700 93. Project CT. The COVID-19 tracking project 2020 [May 1]. Available from: [https://covidtracking.com/about-](https://covidtracking.com/about-project)  
701 [project](https://covidtracking.com/about-project).
- 702 94. Buchanan L, Lai KKR, McCann A. U.S. Lags in Coronavirus Testing After Slow Response to Outbreak. The  
703 New York Times. 2020 March 17.
- 704 95. Y L, S F, S F. The contribution of pre-symptomatic infection to the transmission dynamics of COVID-2019  
705 [version 1; peer review: 3 approved]. Wellcome Open Research. 2020;(5):58. doi: 10.12688/wellcomeopenres.15788.1.
- 706 96. Moghadas SM, Fitzpatrick MC, Sah P, Pandey A, Shoukat A, Singer BH, et al. The implications of silent  
707 transmission for the control of COVID-19 outbreaks. Proceedings of the National Academy of Sciences.  
708 2020;117(30):17513-5. doi: 10.1073/pnas.2008373117.
- 709 97. Wei WE, Li Z, Chiew CJ, Yong SE, Toh MP, Lee VJ. Presymptomatic Transmission of SARS-CoV-2 —  
710 Singapore, January 23–March 16, 2020. 2020 April 1. Report No.
- 711 98. Mizumoto K, Kagaya K, Zarebski A, Chowell G. Estimating the asymptomatic proportion of coronavirus  
712 disease 2019 (COVID-19) cases on board the Diamond Princess cruise ship, Yokohama, Japan, 2020. Euro surveillance  
713 : bulletin Europeen sur les maladies transmissibles = European communicable disease bulletin. 2020;25(10):2000180.  
714 doi: 10.2807/1560-7917.ES.2020.25.10.2000180. PubMed PMID: 32183930.
- 715 99. Mayorga L, García Samartino C, Flores G, Masuelli S, Sánchez MV, Mayorga LS, et al. Detection and  
716 isolation of asymptomatic individuals can make the difference in COVID-19 epidemic management. medRxiv.  
717 2020:2020.04.23.20077255. doi: 10.1101/2020.04.23.20077255.
- 718 100. Desarrollo Ud. UDD study seeks to determine Covid-19 prevalence in the Metropolitan Region. School of  
719 Medicine, German clinic development university  
720 . 2020 May 25.
- 721 101. Tindale L, Coombe M, Stockdale JE, Garlock E, Lau WYV, Saraswat M, et al. Transmission interval estimates  
722 suggest pre-symptomatic spread of COVID-19. medRxiv. 2020:2020.03.03.20029983. doi: 10.1101/2020.03.03.20029983.
- 723 102. Wiersinga WJ, Rhodes A, Cheng AC, Peacock SJ, Prescott HC. Pathophysiology, Transmission, Diagnosis,  
724 and Treatment of Coronavirus Disease 2019 (COVID-19): A Review. JAMA. 2020;324(8):782-93. doi:  
725 10.1001/jama.2020.12839.
- 726



728



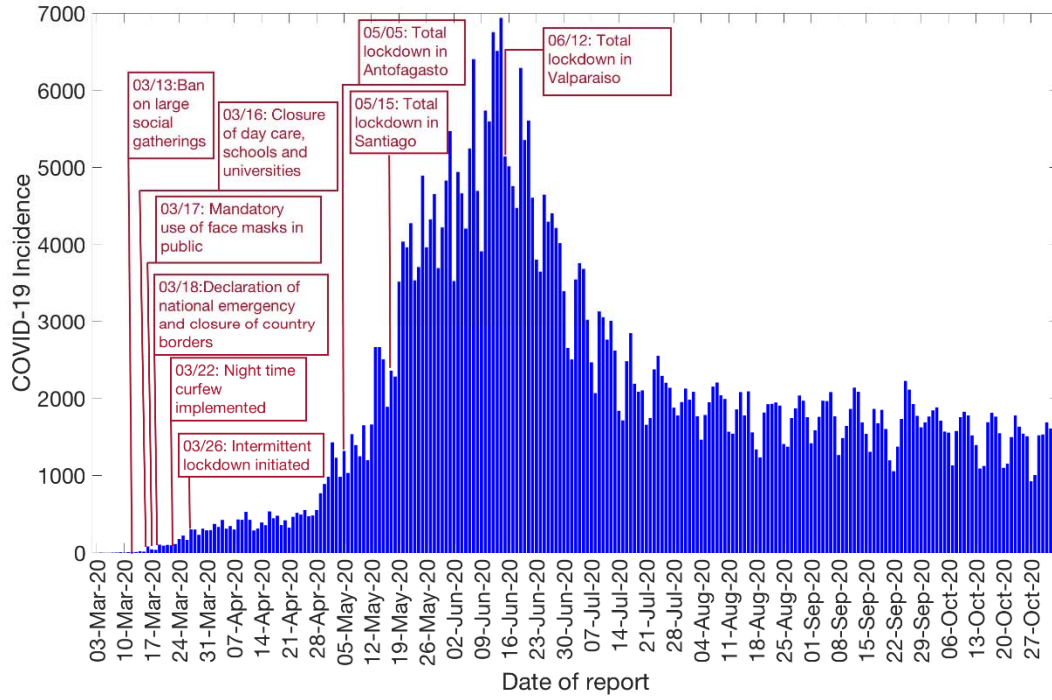
729

730 Figure 1: Timeline of the milestones COVID-19 pandemic in Chile as of November 2<sup>nd</sup>, 2020.

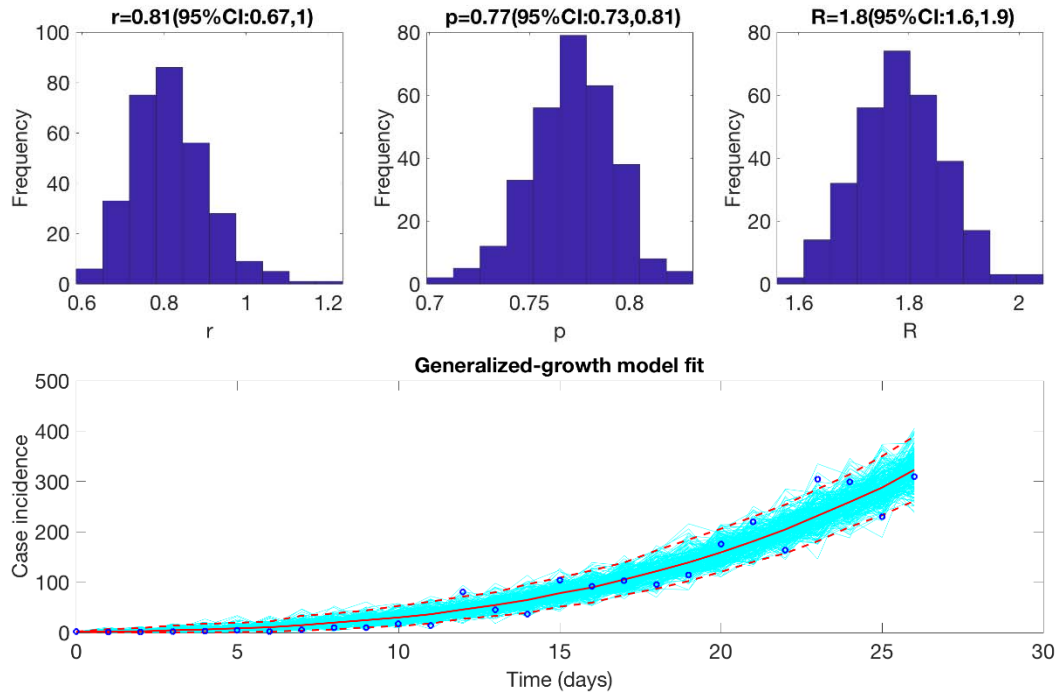
731

It is made available under a [CC-BY 4.0 International license](https://creativecommons.org/licenses/by/4.0/).

732



737



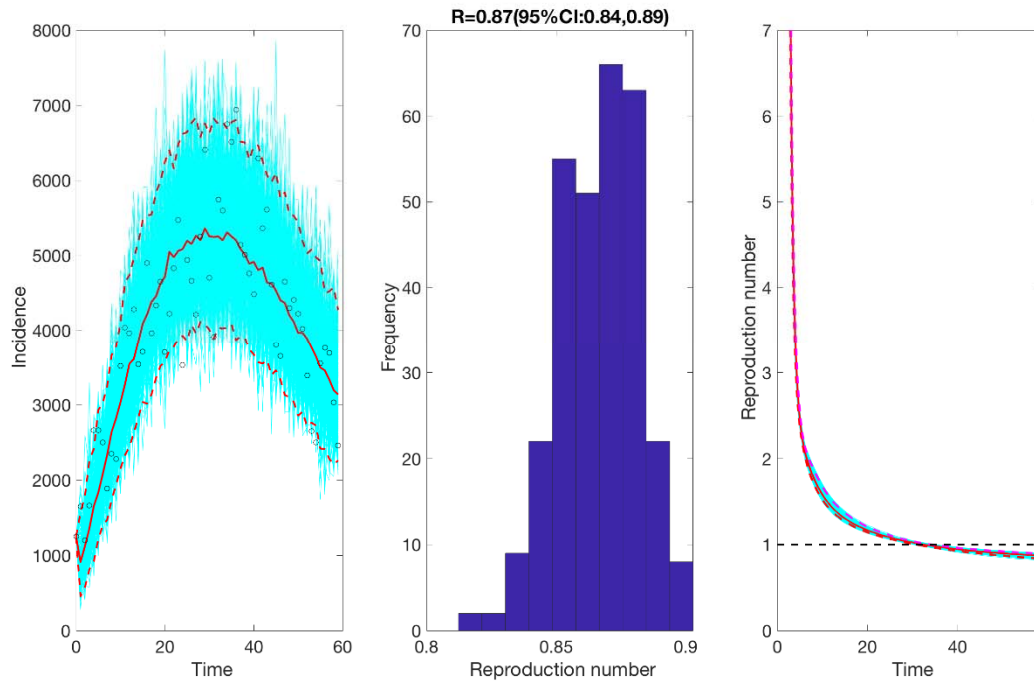
738

739 Figure 3: Reproduction number with 95% CI estimated using the GGM model. The estimated  
740 reproduction number of the COVID-19 epidemic in Chile as of March 28<sup>th</sup>, 2020, is 1.8 (95% CI: 1.6,  
741 1.9).

742

743

744



745

746

747 Figure 4: Reproduction number with 95% CI estimated by calibrating the GLM model from May 9<sup>th</sup>-July

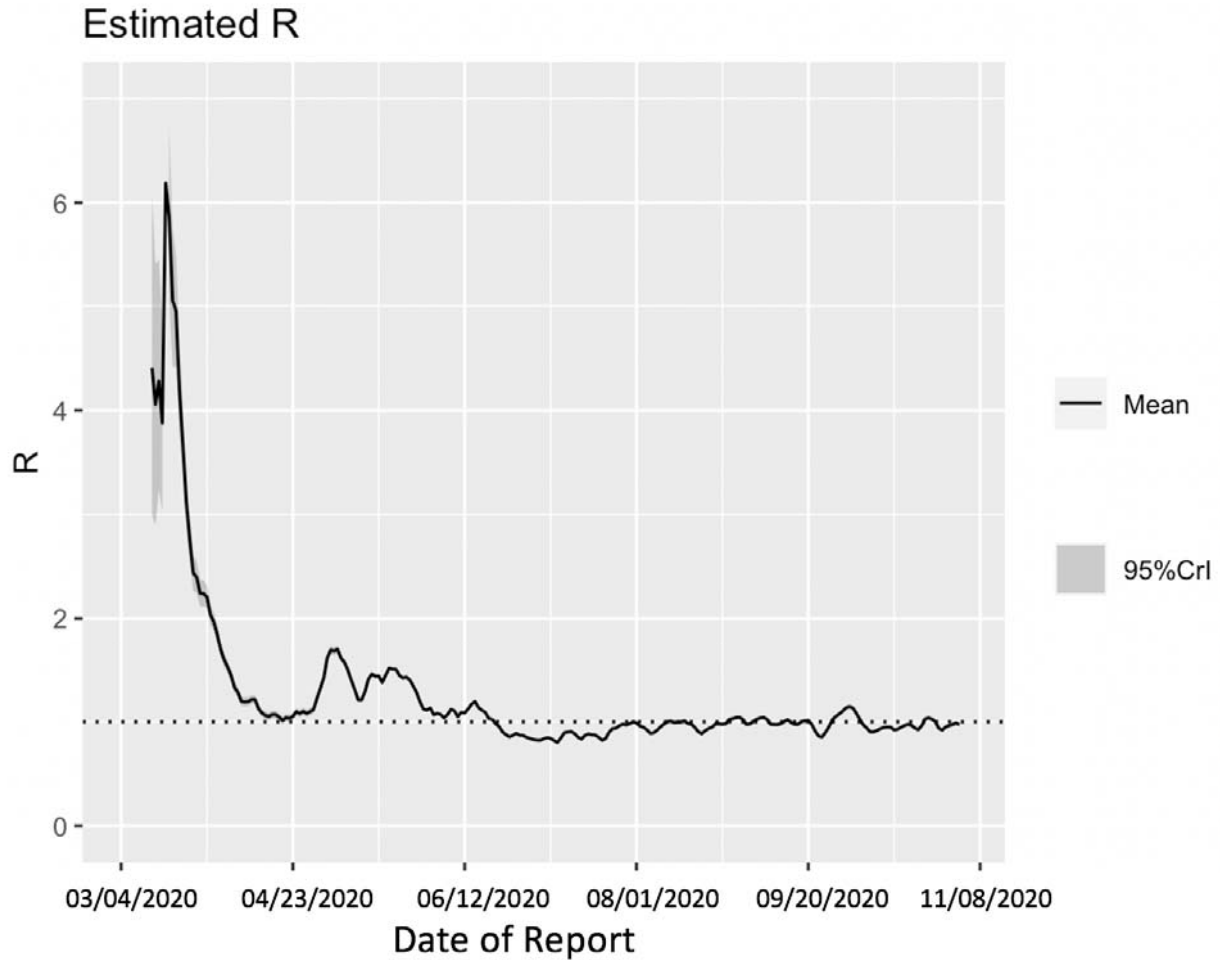
748 7<sup>th</sup>, 2020. The estimated reproduction number of the COVID-19 epidemic in Chile as of July 7<sup>th</sup>, 2020, is

749 0.87 (95% CI: 0.84, 0.89).

750

751

752



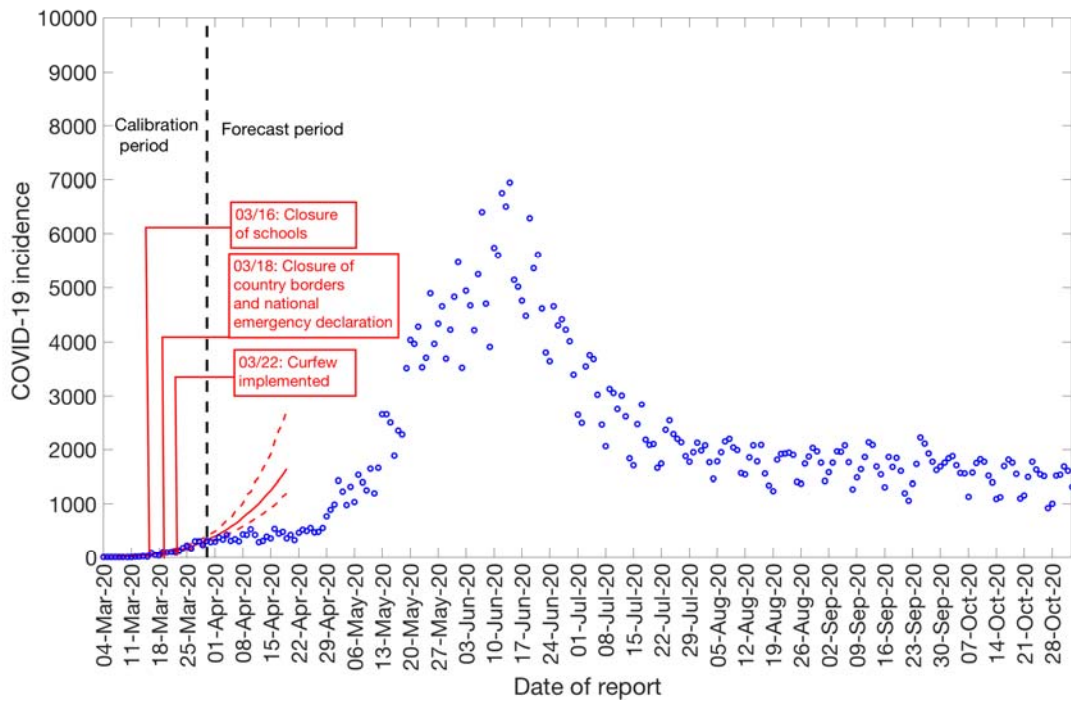
753

754 Figure 5: Estimate of instantaneous reproduction number ( $R$ ) for the COVID-19 epidemic in Chile as of  
755 November 2<sup>nd</sup>, 2020 using the Cori method. The most recent estimate of  $R \sim 0.96$  (95% CrI: 0.95, 0.98) as  
756 of November 2<sup>nd</sup>, 2020. Black solid line represents the mean  $R$  and the gray shaded region represents the  
757 95% credible interval around mean  $R$ .

758

759



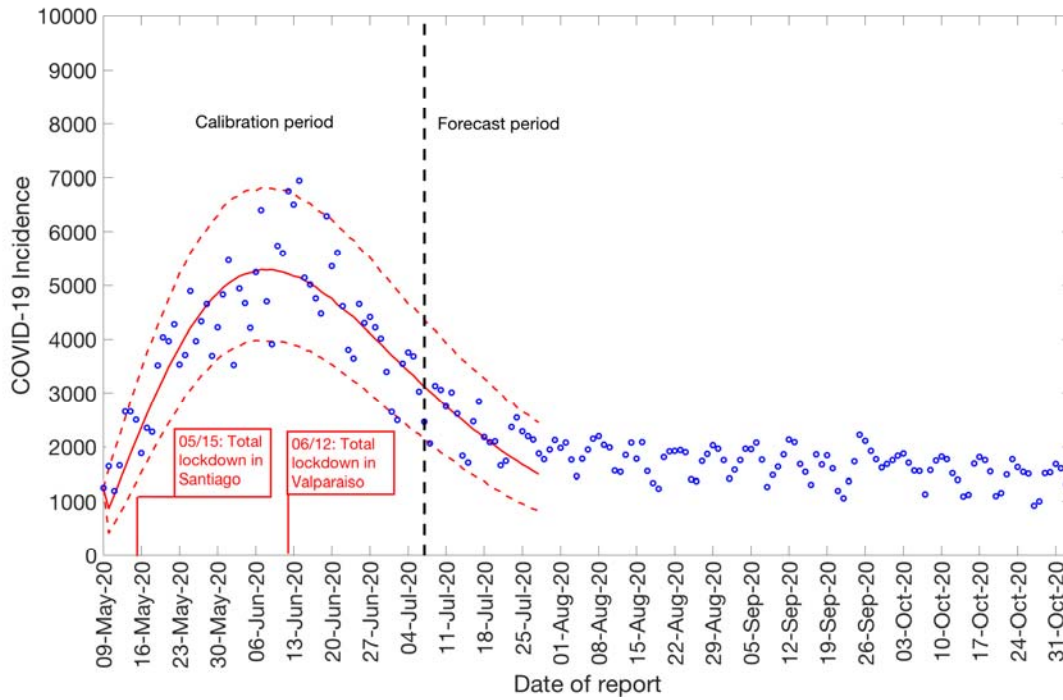


760

761 Figure 6: 20-days ahead forecast of the COVID-19 epidemic in Chile by calibrating the GGM model until  
762 March 30<sup>th</sup>, 2020. Blue circles correspond to the data points; the solid red line indicates the best model fit,  
763 and the red dashed lines represent the 95% prediction interval. The vertical black dashed line represents  
764 the time of the start of the forecast period.

765

766



767

768 Figure 7: 20-days ahead forecast of the COVID-19 epidemic in Chile by calibrating the GLM model from

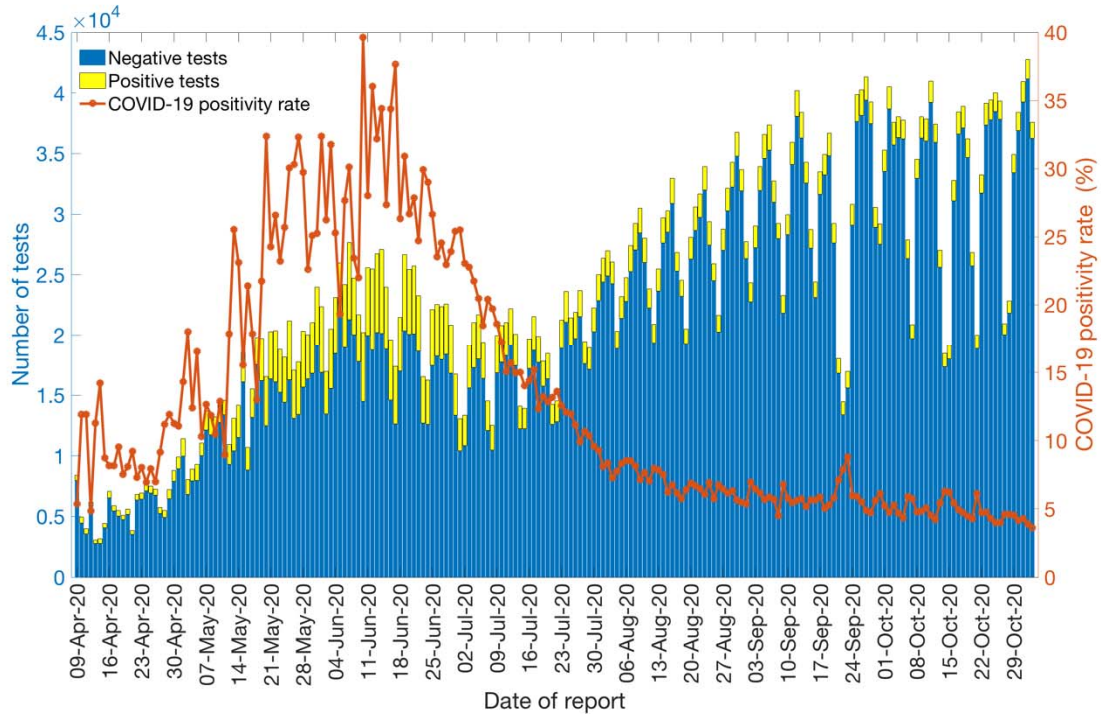
769 May 9<sup>th</sup>-July 7<sup>th</sup>, 2020. Blue circles correspond to the data points; the solid red line indicates the best

770 model fit, and the red dashed lines represent the 95% prediction interval. The vertical black dashed line

771 represents the time of the start of the forecast period. (96.2 is variance)

772

773



774

775 Figure 8: Laboratory results for the COVID-19 tests conducted in Chile as of November 2<sup>nd</sup>, 2020. The

776 blue color represents the negative test results, and the yellow color represents the positive test results. The

777 solid orange line represents the positivity rate of COVID-19 in Chile.

778

779